This full text paper was peer reviewed at the direction of IEEE Communications Society subject matter experts for publication in the IEEE Globecom 2011 proceedings.

Discerning Direct and Indirect Paths: Principle and Application in Passive Target Positioning Systems

Junyang Shen, *Student Member, IEEE* and Andreas F. Molisch, *Fellow, IEEE*

***Abstract*—Passive target localization is an important prerequisite for applications ranging from security to logistics to emergency response. The localization system estimates the location of the target by utilizing runtime and direction of the signal (multipath component, MPC) *directly* reflected by the target. Indirect paths (IPs), i.e., MPCs that interact with environmental objects as well as the target, need to be discerned from the direct paths; failing to do so brings bias to location estimate, and is a major source of localization error. This paper proposes a novel scheme for the detection of IPs in the presence of noise, jointly employing the time of arrival (TOA), direction of arrival (DOA) and direction of departure (DOD) estimates. The decision statistic of this scheme is the distance between the intersection of DOA and DOD directions and the TOA ellipse. Under the assumption of Gaussian errors of TOA, DOA and DOD, the scheme is implemented to maximize the probability of detection given a fixed probability of false alarm. The paper derives closed-form equations for the decision criterion and the resulting performance. Simulation results are given to support the validity of our scheme.**

***Index Terms*—TOA, DOD, DOA, Indirect Path Detection**

I. Introduction

Radio positioning technologies supply location information of objects/targets and have recently received a large amount of attention for various applications, such as patient monitoring, survivor localization in emergency rescue operations and node positioning in sensor networks [1].

The target to be localized can be either "active", transmitting signals, or "passive", only reflecting signals from a seperate source. Active target positioning scenarios includes cell phone location estimation or wireless sensor positioning in the IEEE 802.15.4a Wireless Sensor Networks (WSNs). The passive target positioning scenario is also typical in many applications such as survivor rescue, anti-theft surveillance, automated environment mapping. Radar is also a "passive" localization technology which has been studied for many years [2]. The 'passive" localization was recently shown to be a promising technology for cancer detection [3].

Radio positioning technologies employ the parameters (such as time of arrival TOA, direction of departure DOD, and direction of arrival DOA) of multipath components propagating between target and the nodes of the localization system (the nodes can be transmitters or receivers). For the subsequent discussion, it is useful to distinguish between the direct path (DP), where the signal propagates directly between the target and the localization system nodes, without interaction with any other objects, and the indirect paths (IP), where the signal interacts with one or more objects/obstacles in addition to the target and system nodes.

Extensive studies [4], [5] show that positioning techniques achieve very accurate location estimate of targets if the DOD, DOA and TOA are obtained for the DP. However, if an IP is mistakenly interpreted as a DP, large errors may occur in the resulting target location estimate.

To combat the negative effects of IPs, various techniques have been proposed in the literature. They can be divided into two categories, IP *mitigation* and IP *detection* [6]. IP mitigation attempts to alleviate or counter the bias of channel parameters introduced by IPs [7], [8], [9], [10], while IP detection attempts to differentiate DPs and IPs so that channel parameters of IPs are not used in the DP based positioning algorithms [11], [12], [13] and [14]. Existing IP identification methods suffer from a dependence on the statistical information of channel parameters, and require knowledge of features of signal impulse responses in various types of environments.

Most importantly, to the best of our knowledge, *most of the existing literature focuses on IP mitigation/detection for the active target situation and little attention has been paid to passive target positioning.* This is all the more critical as there is a fundamental difference between IPs in active and passive localization systems: in an active system, any non-line-of-sight path is an IP path. In passive localization systems, DP implies a single-reflection process (at the target), while IPs undergo multiple reflections. In other words, the detection of IP in passive localization requires the discrimination between single-reflections and multiple-reflections; a task that is fundamentally different from the detection of line-of-sight paths encountered in active systems.

To fill this gap, this paper proposes a new IP detection algorithm based on a TOA, DOD and DOA joint DP detection (TDAJD). TDAJD eliminates the dependence on the signal statistics and impulse response features. The only information needed by TDAJD is the measurements of TOA, DOD and DOA, and the variances of the measurement errors of an MPC; the algorithm then determines whether the MPC is a DP or IP. The TDAJD algorithm is developed under the Neyman-Pearson (NP) criterion so that the probability of detection (PD) is maximized give a fixed probability of false alarm (FA).

The principle of the algorithm is as follows: if there were no measurement errors, any DP would have self-consistent parameters. By this we mean that the DOD-DOA intersection

The authors are with the Department of Electrical Engineering, Viterbi School of Engineering, University of Southern California. Email: {junyangs, molisch}@usc.edu

This paper is partially supported by the office of naval research (ONR) under grant 10599363.

978-1-4244-9268-8/11/$26.00 ©2011 IEEE

point[1] lies on an ellipse corresponding to the TOA[2]. In the presence of measurement errors, the decision statistic of the NP test is the *distance* from the DOA-DOD intersection to the TOA ellipse: if this distance lies below a certain threshold, the algorithm judges the path to be a DP. We first show that for small errors, the intersection of DOD and DOA is a two dimensional Gaussian random variable (RV). Then, we prove that the decision statistic is (one-dimensional) Gaussian and compute its variance. A threshold is then computed, such that comparing the decision variable with this preset threshold, the required probability of a false alarm is achieved while maximizing the detection probability.

The remainder of this paper is organized as follows. Section II presents the system model. The distribution of DOD-DOA intersection and the distance from true target to the TOA ellipse are studied in Section III. The principle of TDAJD is presented in Section IV. Section V presents simulation results of TDAJD. The conclusions are drawn in Section VI.

II. System Model

For simplicity, we consider a two dimensional scenario, as shown in Fig. 1, though extension to three dimensions is straightforward. There is one transmitter at $[-\frac{a}{2}, 0]$, one receiver at $[\frac{a}{2}, 0]$. We assume that estimates of the tuplets of DOA, DOD, and TOA are available, for all MPCs, from array measurements at the TX and RX. Measurement methods and algorithms for the extraction of these MPC parameters (with automatic pairing) are discussed, e.g., in [15], [16]. Without restriction of generality, we consider in the following a single MPC. The target is located at $[p, q]$ and one obstacle (which could give rise to additional interactions) is at $[m, n]$. Then a DP is associated with a tuplet $(\theta_1, \theta_2, p_1 + p_2)$.

In case of a DP, the target location fulfills

$$y = \tan(\theta_{DOD})(x + \frac{a}{2}), \tag{1}$$

$$y = \tan(\theta_{DOA})(x - \frac{a}{2}), \tag{2}$$

$$\frac{x^2}{(\frac{l}{2})^2} + \frac{y^2}{(\frac{l}{2})^2 - (\frac{a}{2})^2} = 1. \tag{3}$$

The target location $[p, q]$ can then easily be estimated based on the measurements of DOD (θ_{DOD}), DOA (θ_{DOA}) and signal travel range (l). Note that $l = c * \text{TOA}$, where c is the speed of light.

[17] and [18] show that in anechoic chamber, with ultra-wide-band signals (2-8 GHz) and sophisticated channel sounding techniques (RIMAX [17]), the standard deviation of TOA (signal travel range) can be less than 0.5 cm, and the standard deviations of DOD and DOA measurements can be less than 0.5 degree. Motivated by these results, as well as for the sake of simplicity, we assume that the TOA, DOD and DOA measurement errors are small and Gaussian distributed.

[1]more precisely, where a straight line passing through the transmitter at an angle equal to the DOD, intersects with a straight line passing through the receiver at an angle equal to the DOA

[2]more precisely, the ellipse with TX and RX in its foci, and total signal runtime (or travel range) equal to the length major axis

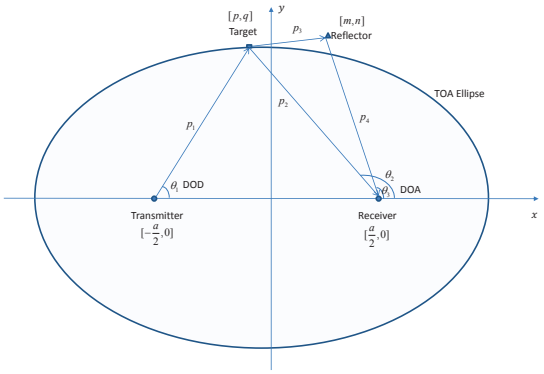

Figure 1. Illustration of TOA, DOA and DOD joint location estimation

An IP involves interaction of the MPC with both the target and additional reflectors, as shown in Fig. 1, resulting in a parameter tuplet $(1; 3; p1 + p3 + p4)$. If the IP detection is not effectively performed, and a target localization (based on Eqs. 1-3) is performed for an IP, large errors can result (we note here that IPs cannot be used for localization at all, since the association between TOA/DOD/DOA and reflector locations is not bijective). If the positioning is based on IP, the mean value of estimated target location by unbiased positioning algorithms is *not* the true target location $[p, q]$ (while for the DP case, the mean value *is* $[p, q]$).

Note that the reflector might be positioned such that interaction with it occurs "on the way" from TX to target; this case can be treated completely analogously. Furthermore, interactions with multiple reflectors are possible, and could be included in our model; however, for the sake of simplicity (and due to the lower power of multiple reflections), we restrict our attention to the case depicted in Fig. 1. MPCs that only interact with environmental reflectors, but not the target, are "background interference" that can be combatted by many techniques well known in radar processing.

In the remainder of this paper, we let $\bar{\bullet}$ denote the true value, $\hat{\bullet}$ denote the estimated or measured value, and $\Delta\bullet = \hat{\bullet} - \bar{\bullet}$.

III. Gaussian Distribution of the DOD and DOA Intersection

In this section, we first prove that for small Gaussian errors of DOD and DOA, the intersection of DOD and DOA is a two dimensional Gaussian random variable. The covariance matrix of the Gaussian distribution is also given. Second, we derive the distribution of the distance from the target to the ellipse of the measured TOA.

A. Distribution of intersection of DOD and DOA

Let θ_1 and θ_2 denote the values of DOD and DOA, see Fig. 1. According to (1) and (2), we obtain $[p, q]$ as follows:

$$p = \frac{a}{2}\frac{\tan(\theta_2) + \tan(\theta_1)}{\tan(\theta_2) - \tan(\theta_1)} = \frac{a}{2}\frac{\sin(\theta_1 + \theta_2)}{\sin(\theta_2 - \theta_1)} \tag{4}$$

$$q = a\frac{\tan(\theta_1\theta_2)}{\tan(\theta_2) - \tan(\theta_1)} = a\frac{\sin\theta_1 \sin\theta_2}{\sin(\theta_2 - \theta_1)} \tag{5}$$

Takeing derivatives of p and q over θ_1 and θ_2, it follows that,

$$\begin{aligned} dp &= \frac{\partial x}{\partial \theta_1} d\theta_1 + \frac{\partial x}{\partial \theta_2} d\theta_2 \\ &= a\frac{\sin\theta_2 \cos\theta_2}{\sin^2(\theta_1-\theta_2)} d\theta_1 - a\frac{\sin\theta_1 \cos\theta_1}{\sin^2(\theta_1-\theta_2)} d\theta_2, \end{aligned} \quad (6)$$

and similarly

$$dq = a\frac{\sin^2\theta_2}{\sin^2(\theta_1-\theta_2)} d\theta_1 - a\frac{\sin^2\theta_1}{\sin^2(\theta_1-\theta_2)} d\theta_2. \quad (7)$$

Under the assumption that the deviation of estimated from true target location, Δp and Δq, are small, we can substitute them into (6) and (7). From this, we can obtain $\Delta\theta_1$ and $\Delta\theta_2$ as functions of Δp and Δq as follows:

$$\begin{bmatrix} \Delta\theta_1 \\ \Delta\theta_2 \end{bmatrix} = \mathbf{H} \times \begin{bmatrix} \Delta p \\ \Delta q \end{bmatrix}, \quad (8)$$

where,

$$\mathbf{H} = \frac{\sin(\theta_1-\theta_2)}{a} \begin{bmatrix} \frac{\sin\theta_1}{\sin\theta_2} & -\frac{\cos\theta_1}{\sin\theta_2} \\ \frac{\sin\theta_2}{\sin\theta_1} & -\frac{\cos\theta_2}{\sin\theta_1} \end{bmatrix}.$$

Assume that $\Delta\theta_1$ and $\Delta\theta_2$ are two independent Gaussian variables [3] with variance σ_1^2 and σ_2^2. Then, the probability density function (PDF) of $\Delta\theta_1$ and $\Delta\theta_2$ is expressed as

$$\text{Pdf}([\Delta\theta_1, \Delta\theta_2]) = \frac{1}{2\pi\sigma_1\sigma_2} \exp\Big[-\frac{1}{2}\Big(\frac{(\Delta\theta_1)^2}{\sigma_1^2} + \frac{(\Delta\theta_2)^2}{\sigma_2^2}\Big)\Big]. \quad (9)$$

Combining (8) and (9), we obtain the PDF of $[\Delta p, \Delta q]$:

$$\begin{aligned} \text{Pdf}([\Delta p, \Delta q]) &= \frac{1}{2\pi \det^{1/2}|\mathbf{G}|} \times \\ &\exp\left(-\frac{1}{2}[\Delta p,\ \Delta q]\,\mathbf{G}^{-1}\begin{bmatrix} \Delta p \\ \Delta q \end{bmatrix}\right), \end{aligned} \quad (10)$$

where the entries of $\mathbf{G}^{-1}$ are evaluated as follows:

$$\mathbf{G}_{1,1}^{-1} = \frac{\sin^2(\theta_1-\theta_2)}{a^2}\left(\frac{\sin^2\theta_1}{{\sigma_1}^2\sin^2\theta_2} + \frac{\sin^2\theta_2}{{\sigma_2}^2\sin^2\theta_1}\right), \quad (11)$$

$$\begin{aligned} \mathbf{G}_{1,2}^{-1} = \mathbf{G}_{2,1}^{-1} &= -\frac{\sin^2(\theta_1-\theta_2)}{a^2} \times \\ &\left(\frac{\cos^2\theta_1}{{\sigma_1}^2\sin^2\theta_2} + \frac{\cos^2\theta_2}{{\sigma_2}^2\sin^2\theta_1}\right), \end{aligned} \quad (12)$$

$$\mathbf{G}_{2,2}^{-1} = \frac{\sin^2(\theta_1-\theta_2)}{a^2}\left(\frac{\cos^2\theta_1}{{\sigma_1}^2\sin^2\theta_2} + \frac{\cos^2\theta_2}{{\sigma_2}^2\sin^2\theta_1}\right). \quad (13)$$

It is easy to observe from (10) that $[\Delta p, \Delta q]$ is a bivariate Gaussian variable, with covariance matrix $\mathbf{G}$.

[3] correlations of the estimation errors of DOA and DOD could be taken into account in a straightforward manner, but are omitted to simplify notation

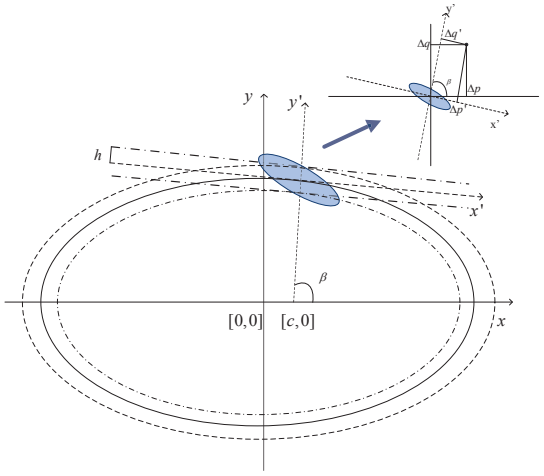

Figure 2. Illustration of DP/IP detection based on distance from DOD-DOA intersection to TOA ellipse

B. Distribution of Distance from True Target to TOA Ellipse

Fig. 2 shows the changes of TOA ellipse due to the TOA measurement error. The solid ellipse is without TOA measurement error, while the dashed and dash-dotted ellipses are with (positive and negative) errors, respectively. Following the standard parametric representation of an ellipse ($x = a cos\alpha$, $y = b sin\alpha$, with a, b major and minor axis, and α running from 0 to 2π), the target location $[p, q]$ can be represented by

$$p = \frac{l}{2}\cos\alpha, \quad (14)$$

$$q = \sqrt{(\frac{l}{2})^2 - (\frac{a}{2})^2}\sin\alpha. \quad (15)$$

Let $\bar{\alpha}$ be the value of α corresponding to the true target location $[\bar{p}, \bar{q}]$ satisfies

$$\tan\bar{\alpha} = \frac{\bar{l}}{\sqrt{\bar{l}^2 - a^2}}\frac{\bar{q}}{\bar{p}}. \quad (16)$$

where $\bar{l}$ denotes the TOA errorless measurement.

Since the true location of the target $[\bar{p}, \bar{q}]$ is unknown, in the remaining of this paper, the estimates of the target location $\hat{p}$ and $\hat{q}$ are used. $\hat{p}$ and $\hat{q}$ are evaluated as $\hat{p} = \frac{p_1+p_2+p_3}{3}$ and $\hat{q} = \frac{q_1+q_2+q_3}{3}$, where $[p_1, q_1]$ is the solution of (1)-(2), $[p_2, q_2]$ is the solution of (2)-(3) and $[p_3, q_3]$ is the solution of (1)-(3).

We are interested in the relation between the location change of the target $[\Delta p, \Delta q]$ and the change of the TOA measurement Δl. Taking the derivative of (14) and (15) with respect to l and substituting Δp, Δq, and Δl for dp, dq, and dl, we obtain

$$\tan\beta = \frac{\Delta q}{\Delta p} = \frac{\hat{l}}{\sqrt{(\hat{l}^2 - a^2)}}\tan\hat{\alpha}. \quad (17)$$

where $\hat{\alpha}$ denotes the estimated value and $\hat{l}$ denotes the measured value. (17) means as the TOA measurement changes, the perpendicular line from the true target location to the TOA ellipse has the slope $\tan\beta$.

The tangent line of the ellipse at the target point is

$$\frac{\hat{p}x}{(\frac{\hat{l}}{2})^2} + \frac{\hat{q}y}{(\frac{\hat{l}}{2})^2 - (\frac{a}{2})^2} = 1. \quad (18)$$

The slope value of the tangent line is

$$\tan\gamma = -\frac{\hat{l}^2 - a^2}{\hat{l}^2}\frac{\hat{p}}{\hat{q}}. \quad (19)$$

which obviously fulfills the condition $\tan\beta\tan\gamma = -1$.

We can further calculate the intersection of the perpendicular line and the x axis at $[c, 0]$, where

$$c = \frac{a^2}{2\hat{l}}\cos\hat{\alpha}. \quad (20)$$

Remarks: Our derivation above implies that the distance from the true target to the TOA ellipse can be approximated by the distance from the true target to the tangent line of the TOA ellipse. Besides, for different TOA measurements with small differences, their tangent lines can be considered to be parallel with each other, as shown in Fig. 2.

IV. Principle of TDAJD

In this section, we first propose the idea of TDAJD, based on the distance from the DOD-DOA intersection to the TOA ellipse, then analyze the decision statistics and derive the threshold value given the required probability of false alarm (PF).

As shown in Fig. 2, the DP/IP discrimination is based on the distance from the DOD-DOA intersection to the tangent line of the TOA ellipse. The DOD-DOA intersection is a two-dimensional random variable, which is indicated by the small shadowed ellipse in the figure. If the distance from the DOD-DOA intersection to the TOA ellipse z is less than a threshold h, the detection algorithm claims that it is a DP, otherwise, the detection algorithm claims that it is an IP. To evaluate the performance of detection algorithm, the two commonly used metrics are the probability of false alarm (PF) and the probability of detection (PD).

The PF denotes the probability that the algorithm claims an IP when the channel is actually a DP, which is expressed as follows:

$$\begin{aligned} P_f &= \text{Prob(The algorithm claim a IP | The path is a DP)} \\ &= \text{Prob}(z > h \mid \text{The channel is a DP}), \end{aligned}$$

and the PD denotes the probability that the algorithm claims a IP when the channel is actually a IP, which is expressed as follows:

$$\begin{aligned} P_d &= \text{Prob(The algorithm claim a IP | The path is a IP)} \\ &= \text{Prob}(z > h \mid \text{The channel is an IP}). \end{aligned}$$

It is easy to observe that P_f is independent of the location of the obstacles/reflectors while P_d is not.

For analytical convenience, we set up a new coordinate system where the new x axis is the true tangent line of the TOA at the target location and the new y axis is the perpendicular line of the TOA ellipse at the true target location. The new x and y axes are shown in Fig. 2 by x' and y' with dashed line. Let the location of the target in the new x'-y' system be $[p', q']$.

Assume the intersection between the tangent of the *measured* ellipse and the y' axis is at $(x', y') = (0, s)$, and the PDF of the DOD-DOA intersection location in the new coordinate system be $\text{Pdf}(p', q')$. The probability that the distance between the DOD/DOA intersection location to the tangent line of the measured TOA ellipse is smaller than h, is evaluated as

$$\xi(s) = \int_{s-h}^{s+h}\int_{-\infty}^{\infty} \text{Pdf}(p', q')dp'dq'. \quad (21)$$

P_f is the probability that the distance from DOD-DOA intersection to tangent line is larger than h when the channel is a DP. Let $\eta(s)$ denote the probability density function (PDF) of s, considering all the possible value of s, P_f is then evaluated as

$$P_f = 1 - \int_{-\infty}^{\infty}\eta(s)\int_{s-h}^{s+h}\int_{-\infty}^{\infty} \text{Pdf}(p', q')dp'dq'ds. \quad (22)$$

The rest of this section studies the evaluations of $\eta(s)$ and $\text{Pdf}(p', q')$, P_f and P_d, respectively.

A. Evaluation of $\eta(s)$

Let d_1 denote the distance from $[c, 0]$ to the TOA ellipse, and $\Delta d_1 = s$ denote the change of d_1 due to the change of TOA measurement l.

According to (14) and (15),

$$\begin{aligned} d_1 &= \sqrt{\Big(\frac{l}{2}\cos\alpha - c\Big)^2 + \Big(\sqrt{(\frac{l}{2})^2 - (\frac{a}{2})^2}\sin\alpha\Big)^2} \\ &= \sqrt{\frac{l^2}{4} - lc\cos\alpha - \frac{a^2}{4}\sin^2\theta} \end{aligned} \quad (23)$$

Then, for small value of Δl, s or Δd_1 can be expressed as

$$s = \Delta d_1 = \Big(\frac{\frac{l}{4} - \frac{c}{2}\cos\alpha}{d_1}\Big)\Delta l. \quad (24)$$

(24) indicates that s is Gaussian distributed under the assumption that Δl is a Gaussian random variable with PDF

$$\eta(s) = \frac{1}{\sqrt{2\pi\text{var}(s)}}\exp\Big(-\frac{s^2}{2\text{var}(s)}\Big), \quad (25)$$

where

$$\text{var}(s) = \Big(\frac{\partial d_1}{\partial l}\Big)^2\text{var}(l) = \left(\frac{\frac{l}{4} - \frac{c}{2}\cos\alpha}{d_1}\right)^2\text{var}(l). \quad (26)$$

B. Evaluation of $p(x', y')$

As shown in Fig. 2, the origin in the new coordinate system is first moved to the true position of target. β denotes the anticlockwise angle from x axis to y' axis. Starting with (10), and considering the effect of coordinate rotation, the resulting PDF is again a two-dimensional Gaussian distribution with covariance matrix $\mathbf{G}'$, denoted by $\mathbf{G}' = \mathbf{KGK^{-1}}$ where

$$\mathbf{K} = \begin{bmatrix} \sin\beta & -\cos\beta \\ \cos\beta & \sin\beta \end{bmatrix}. \quad (27)$$

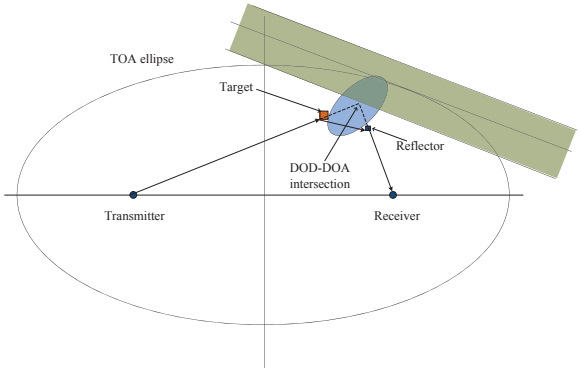

Figure 3. Illustration for P_d calculation

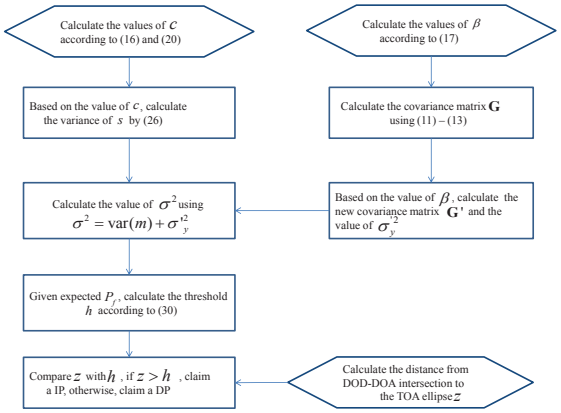

Figure 4. Flow chart of proposed algorithm

The PDF of $[x', y']$ is

$$\mathrm{Pdf}([p', q']) = \frac{1}{2\pi \det^{1/2} |\mathbf{G}'|} \times \exp\left(-\frac{1}{2}[p',\ q']\,\mathbf{G}'^{-1}\begin{bmatrix} p' \\ q' \end{bmatrix}\right). \quad (28)$$

The variances of the location of DOD-DOA intersection in the new coordinate system are $\mathrm{var}(p') = \mathbf{G}'(1,1)$ and $\mathrm{var}(q') = \mathbf{G}'(2,2)$.

C. Evaluation of P_f

Starting with (22), (25) and (28), and using some straightforward manipulations, P_f can be simplified to

$$P_f = 1 - \int_{-h}^{h} \frac{1}{\sqrt{2\pi\sigma^2}} \exp\Big(-\frac{r^2}{2\sigma^2}\Big) dr = 2Q\Big(\frac{h}{\sigma}\Big). \quad (29)$$

where $Q(x) = \frac{1}{\sqrt{2\pi}} \int_x^\infty \exp(-\frac{u^2}{2}) du$ and $\sigma^2 = \mathrm{var}(s) + \mathrm{var}(y')$. Therefore, to achieve the expected P_f, the threshold h is

$$h = \sigma Q^{-1}\Big(\frac{P_f}{2}\Big). \quad (30)$$

The expected PF can be achieved by the preset threshold h from (30).

D. Evaluation of P_d

The value of P_d depends on the distribution of the location of the reflectors. As a simple example, Fig. 3 shows the situation when there is only one reflector. The shadowed ellipse and rectangle denote the DOD-DOA intersection and area where the distance to the tangent line of TOA ellipse is smaller than h, respectively. If the estimated location falls into the overlap region, the path is interpreted as DP, even though a double reflection has occurred. In other words, the probability of detection of an IP is P_d =Prob(The DOD-DOA intersection is outside of the shadowed rectangle | The channel is an IP).

In Fig. 3 , we can also interpret $1 - P_d$ as the overlapping area between the shadowed ellipse and rectangle. More overlapping between the shadowed ellipse and rectangle means smaller P_d.

Note that based on system requirements, P_f and P_d may have different definitions. More details about various definitions of P_f and P_d are presented in [19]. The evaluation of P_d requires the evaluation of a triple integral, which is not shown here due to space restrictions; it depends on the PDF of the location of reflectors. For certain PDFs, a simplification of the integral is possible; more details are presented in [19]. An extension of TDAJD is proposed in [19] to deal with general non-Gaussian distributions of DOD, DOA and TOA measurements.

V. Simulation Results

In this section we evaluate the performance of the algorithm. An overall flowchart is shown in Fig. 4.

Fig. 5 (a)-(c) exhibit P_d vs P_f curves with different simulation settings. A threshold is calculated *a priori*, using (30), to achieve the expected value of P_f. Then, based on the threshold, the values of P_d and P_f obtained by numerical simulations are shown in the figure. To show the impact of different reflector location, we assume the reflector is randomly distributed. Particularly, if the target is at $[x, y]$, there is one reflector location uniformly distributed in the range $[x - w, x + w] \bigcap [y - w, y + w]$.

The simulation results show that the proposed algorithm effectively detects the IP with high PD and low PF, when the TOA, DOD and DOA errors are small, which is achievable with sophisticated channel sounding technique and ultra wideband signals [17], [18] and [20].

Several phenomenons deserving notice are

1) **Impact of angle error** (Fig. 5 (a)): In our setting, the change of DOD error variance has larger impact on P_d than the change of DOA error variance. This is because the distance between the transmitter and the target is larger than the distance between the receiver to the target, therefore, change of DOD introduces larger variation to the DOD-DOA intersection than the change of DOA.
2) **Impact of w** (Fig. 5 (b)): Larger w leads to higher P_d. This is because larger w leads to larger average distance between the target and reflector, resulting in higher probability of discerning an IP and DP.

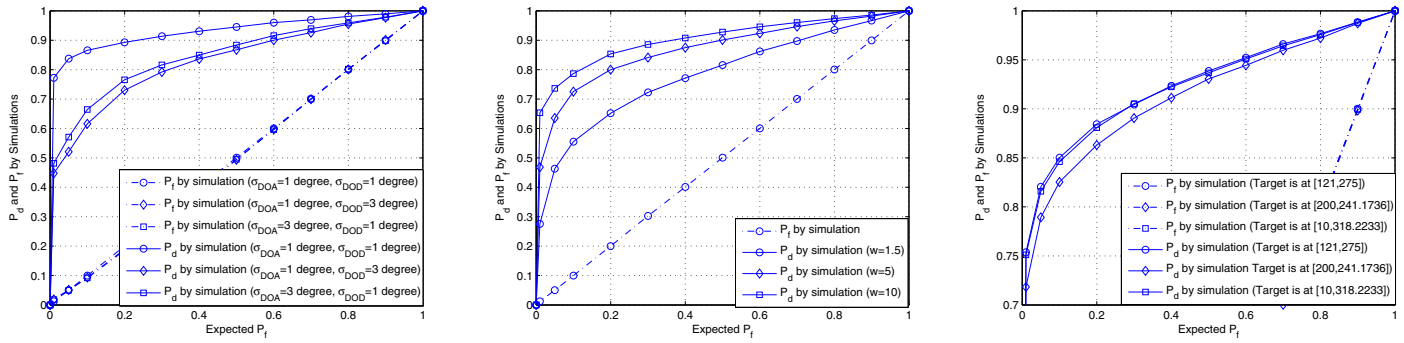

(a) (b) (c)

Figure 5. (a), Simulation results various DOD and DOA values (target is at $[4, 6]$, $a = 4$, $w = 4$ and $\sigma_{TOA} = 0.03$); (b), Simulation results with various values of w (target is at $[8, 10]$, $a = 4$, $\sigma_{TOA} = 0.02, \sigma_{DOA} = 0.8$ degree, $\sigma_{DOD} = 1.2$ degree); (c), Simulations results with various target locations ($a = 100$, $w = 50$, $\sigma_{TOA} = 0.005$, $\sigma_{DOA} = 0.7$ degree, $\sigma_{DOD} = 0.4$ degree).

Table I
LIST OF DISTANCES BETWEEN TARGET AND TRANSMITTER/RECEIVER

	Distance to Transmitter	**Distance to Receiver**
$[121, 275]$	323.8302	284.0176
$[200, 241.1736]$	347.3683	284.0176
$[10, 318.2233]$	323.8302	320.7274

3) **Impact of target location** (Fig. 5 (c)): The distances between the target and transmitter/receiver are shown in Table I. The simulation results in Fig. 5 (c) indicate that larger distance from the target to the transmitter or receiver leads to smaller P_d. The reason of this phenomenon is the same for the item 1.

VI. CONCLUSION

This paper studied the problem of discriminating IPs and DPs for passive positioning purposes, from a novel perspective. We utilize the TOA, DOD and DOA information together and test whether the parameter tuplet is consistent with the assumption of a DP. In particular, we test the distance between the DOA-DOD intersection point and the TOA ellipse. The algorithm is based on Neyman-Pearson criteria to maximize the probability of detection given probability of false alarm. Simulations show that the algorithm can effectively detect IPs when the TOA, DOD and DOA measurements are available with small errors. The proposed method can be employed to sort out DPs to increase localization accuracy, or identify the IPs to obtain more information about the radio channels.

REFERENCES

[1] S. Gezici, Z. Tian, G. Giannakis, H. Kobayashi, A. Molisch, H. Poor, and Z. Sahinoglu, "Localization via ultra-wideband radios: a look at positioning aspects for future sensor networks," *IEEE Signal Processing Magazine*, vol. 22, no. 4, pp. 70 – 84, July 2005.

[2] A. Tajer, G. Jajamovich, X. Wang, and G. Moustakides, "Optimal joint target detection and parameter estimation by mimo radar," *Selected Topics in Signal Processing, IEEE Journal of*, vol. 4, no. 1, pp. 127 –145, 2010.

[3] M. Klemm, J. Leendertz, D. Gibbins, I. Craddock, A. Preece, and R. Benjamin, "Microwave Radar-Based Differential Breast Cancer Imaging: Imaging in Homogeneous Breast Phantoms and Low Contrast Scenarios," *IEEE Transactions on Antennas and Propagation*, vol. 58, no. 7, pp. 2337 –2344, july 2010.

[4] J.-Y. Lee and R. Scholtz, "Ranging in a dense multipath environment using an uwb radio link," *Selected Areas in Communications, IEEE Journal on*, vol. 20, no. 9, pp. 1677 – 1683, Dec. 2002.

[5] K. Pahlavan, F. O. Akgul, M. Heidari, A. Hatami, J. M. Elwell, and R. D. Tingley, "Indoor geolocation in the absence of direct path," *Wireless Communications, IEEE*, vol. 13, no. 6, pp. 50 –58, 2006.

[6] J. Khodjaev, Y. Park, and A. Saeed Malik, "Survey of NLOS identification and error mitigation problems in UWB-based positioning algorithms for dense environments," *Annals of Telecommunications*, vol. 65, no. 5, pp. 301–311, 2010.

[7] L. Cong and W. Zhuang, "Non-line-of-sight error mitigation in TDOA mobile location," in *Global Telecommunications Conference, 2001. GLOBECOM '01. IEEE*, vol. 1, 2001, pp. 680 –684 vol.1.

[8] M. McGuire and K. Plataniotis, "Dynamic model-based filtering for mobile terminal location estimation," *Vehicular Technology, IEEE Transactions on*, vol. 52, no. 4, pp. 1012 – 1031, 2003.

[9] L. Cong and W. Zhuang, "Nonline-of-sight error mitigation in mobile location," *IEEE Transactions on Wireless Communications*, vol. 4, no. 2, pp. 560 – 573, 2005.

[10] K. Yu and Y. Guo, "Improved positioning algorithms for nonline-of-sight environments," *Vehicular Technology, IEEE Transactions on*, vol. 57, no. 4, pp. 2342 –2353, 2008.

[11] A. Maali, H. Mimoun, G. Baudoin, and A. Ouldali, "A new low complexity NLOS identification approach based on UWB energy detection," in *Radio and Wireless Symposium, 2009. RWS '09. IEEE*, 2009, pp. 675 –678.

[12] K. Yu and Y. Guo, "Statistical NLOS Identification Based on AOA, TOA, and Signal Strength," *Vehicular Technology, IEEE Transactions on*, vol. 58, no. 1, pp. 274 –286, 2009.

[13] S. Marano and, W. Gifford, H. Wymeersch, and M. Win, "Nlos identification and mitigation for localization based on uwb experimental data," *Selected Areas in Communications, IEEE Journal on*, vol. 28, no. 7, pp. 1026 –1035, 2010.

[14] H. Luecken and A. Wittneben, "UWB radar imaging based multipath delay prediction for NLOS position estimation," in *IEEE International Conference on Ultra-Wideband, ICUWB 2011*, Sep. 2011.

[15] A. Richter, "Estimation of Radio Channel Parameters: Models and Algorithms," Ph. D. dissertation, Technischen Universität Ilmenau, Germany, May 2005, ISBN 3-938843-02-0.

[16] A. F. Molisch, *Wireless Communications*, 2nd ed. Wiley, 2011.

[17] J. Salmi and A. F. Molisch, "Propagation parameter estimation, modeling and measurements for ultrawideband MIMO radar," *to appear in IEEE Transactions on Antennas and Propagation*, 2011, in press.

[18] J. Shen and A. F. Molisch, "Passive Location Estimation Using TOA Measurements," *to appear IEEE International Conference on Ultra-Wideband (ICUWB)*, 2011.

[19] ——, "Geographic based Indirect Path Detection: Principles and Applications in Target Positioning Systems," *manuscript in preparation*, 2011.

[20] J. Shen, A. F. Molisch, and J. Salmi, "Accurate Passive Location Estimation Using TOA Measurements," *submitted to IEEE Transactions on Wireless Communications*, 2011.